Int. J. Electrochem. Sci., 17 **(2022)** Article Number: 221031, doi: 10.20964/2022.10.43

International Journal of ELECTROCHEMICAL SCIENCE
www.electrochemsci.org

Reaction and Kinetics Studies of Immobilized Enzyme Systems: PartII With External Mass Transfer Resistance

M. Sivakumar[1], *R. Senthamarai*[2,*], *L. Rajendran*[3], *M.E.G. Lyons*[4]

[1] Department of mathematics, College of Science and Humanities, SRM Institute of Science and Technology, Vadapalani, Chennai, India.
[2] Department of Mathematics, College of Engineering and Technology, SRM Institute of Science and Technology, Kattankulathur – 603 203, Tamilnadu, India.
[3] Department of Mathematics, Academy of Maritime Education and Training (AMET) Deemed to be University, India.
[4] School of Chemistry & AMBER National Centre, University of Dublin, Trinity College Dublin, Ireland
[*]E-mail: senthamr@srmist.edu.in

Received: 6 July 2022 / *Accepted:* 22 August 2022 / *Published:* 10 September 2022

In this present work, nonlinear reaction-diffusion equations in immobilized enzyme reactions have been solved analytically to estimate the substrate concentrations for the case of external mass transfer resistance for various geometrical shapes, such as planar, cylindrical and spherical forms of particle substrates. Taylor's series method is applied for an analytical approximation of the dimensionless substrate concentration on immobilized enzyme reactions. The analytical solution is compared with the numerical solution result using MATLAB software coding and graphs for solving the boundary value problems. The effectiveness factor (*Ef)* values have also been estimated and tabulated for the three geometries handled herein to describe the mass transfer limitation effect on the overall reaction rate. The Taylor series converges rapidly and yields an exact and readily verifiable series of analytic approximations for various relevant reaction parameters involved in this boundary value problem.

Keywords: Mathematical modelling, Nonlinear reaction-diffusion equations, Taylor series method, Michaelis–Menten kinetics, Immobilized enzyme reactions

1. INTRODUCTION

In the immobilization of enzymes, several factors affect the observed kinetics, such as interparticle and intraparticle diffusion limitations, the partitioning of the substrate between the support and bulk of the solution, conformation and spatial effects due to the immobilization mechanism. The consequences of such immobilizations result in disfiguration of the enzyme, and due to this, the substrate's flux may be resisted, and concentration levels of the substrate vary. These effects depend on

the properties of the support, the substrate and its concentration, and the immobilization procedure [1, 2]. The mass transfer limitation effects on the observed reaction rates are due to the external mass transfer resistance of the substrate from the bulk fluid phase to the external surface of the support particle substrates and internal mass transfer resistance due to pore diffusion [3, 4].

In [5,6], an optimization algorithm was applied for the estimation of several substrate mass transfer parameters, including the effective diffusivity of the substrate within the support particle substrates and the overall external mass transfer coefficient, based on the experimental data under irreversible uni-reactant immobilized enzyme systems. In this paper, the mathematical model [7] has been solved for the dimensionless substrate concentration profile for the case with external mass transfer resistance using Taylor's series method for various geometrical shapes of the catalyst particle substrates, viz. planar, cylindrical and spherical, and the results have been tabulated and shown the variations of the concentration levels graphically for these three cases, and the effectiveness factor variations for various values of the parameters have been found and tabulated.

Nomenclature

Parameter	Meaning	Unit (Planar)	Unit (Others)
S	Substrate Concentration	(kg/m^3)	(µmol/cm^3)
D_e	Effective diffusivity of the substrate in the particle substrate	(m^2/s)	(m^2/s)
K_m	Michaelis constant	(*kg*/m^3)	(µmol/cm^3)
v	Reaction rate	(kg/s/m^3 cat)	(µmol/min/cm^3 cat)
V_m	Maximum reaction rate	(kg/s/m^3 cat)	(µmol/min/cm^3 cat)
S_b	Substrate concentration in the bulk fluid phase	(kg/m^3)	(µmol/cm^3)
k_l	External mass transfer coefficient	(m/s)	(m/s)
R	Half-thickness of the particle substrate	(m)	(m)
B_i	Biot number	(None)	(None)
g	Particle substrate shape factor	(None)	(None)
$C(X)$	Dimensionless substrate concentration	(None)	(None)
X	Dimensionless distance from the center tothe surface of symmetry of the particle substrate	(None)	(None)
x	Distance from the centre to the surface of symmetry of the particle substrate	(None)	(None)
β	Dimensionless substrate concentration under Michaelis kinetics	(None)	(None)
α	Theile Modulus	(None)	(None)

2.MATHEMATICAL FORMULATION OF THE MODEL

The kinetic model of immobilized enzymes is based on the following assumptions [3]*:* (i) The model of immobilized enzymes is described by Michaelis–Menten kinetics in irreversible processes. (ii) The inner surface of the particle substrate support has a uniform distribution of enzymes fixed to it. (iii) The impact of the partition from the bulk fluid phase to the support of the particle is neglected. (iv)

Inside the support, the temperature and the effective diffusivity remain constant. (v) Enzyme deactivation is disregarded. 6. It should only take into account the steady-state conditions that were in place.

The enzymes are evenly active, and substrate diffusion occurs in a thin fluid phase surrounding the support surface and reaches the reactive surfaces of the enzymes adsorbed on the support, as depicted in Figure 1. All enzyme molecules are equally active, and the substrate diffuses through a thin fluid phase surrounding the support surface to reach the reactive surfaces of adsorbed enzymes, as depicted in Figure 1.

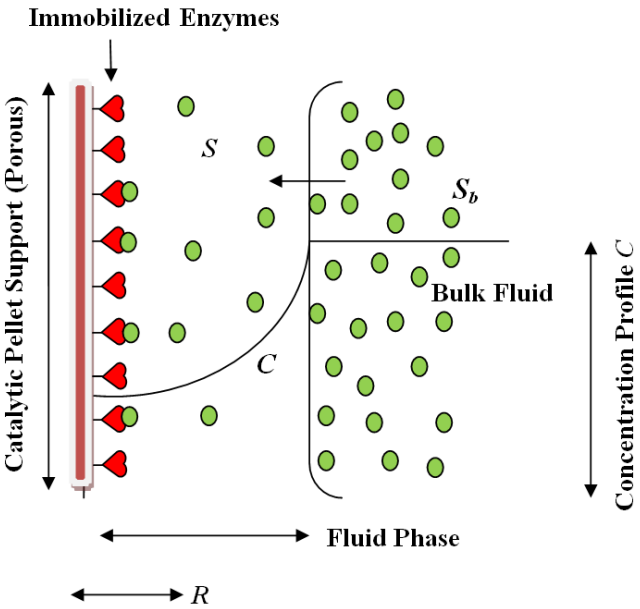

Figure 1. Schematic representation of the immobilized enzyme system

The differential equation and its boundary conditions express the dimensionless substrate concentration, *C*, in the particle substrate [3]:

$$\frac{d^2C}{dX^2}+\frac{g-1}{X}\frac{dC}{dX}=\alpha^2\frac{C}{1+\beta C} \tag{1}$$

at $X = 0$: $\frac{dC}{dX}=0$ (2)

at $X = 1$: $\frac{dC}{dX}=B_i(1-C)$ (with external mass transfer resistance) (3)

where *X* is the dimensionless distance to the center or the surface of symmetry of the particle substrate and g is the particle substrate shape factor. The dimensionless parameters are defined as follows:

$$C=\frac{S}{S_b},\ X=\frac{x}{R},\ \beta=\frac{S_b}{K_m},\ \alpha=R\sqrt{\frac{V_m}{K_mD_e}}\ \text{(Thiele Modulus) and}\ B_i=R\frac{k_l}{D_e}\ \text{(Biot number)} \tag{4}$$

To describe the mass transfer limitation effect on the overall reaction rate, the overall effectiveness factor, η, is the ratio of the reaction rate and reaction rate in the absence of internal and external resistance. The effectiveness factor is obtained by differentiating the concentration profile for which the substrate concentration is taken in the bulk fluid phase, as follows:

$$\eta = \frac{g(1+\beta)}{\alpha^2}\left(\frac{dC}{dX}\right)_{at\ X=1} \tag{5}$$

3. AN ANALYTICAL EXPRESSION FOR THE SUBSTRATE CONCENTRATION AND EFFECTIVENESS FACTOR (η) ON IMMOBILIZED ENZYME REACTIONS USING TAYLOR SERIES METHOD

From a mathematical point of view, the best approximation of a function of the boundary value problem has a vital role in its application. There are several analytical and numerical methods in our mathematical modelling field to deal with nonlinear models and their solutions subject to the given boundary conditions, such as the variational iteration method (VIM) [8,9], Taylor's series method [10-18], modified Adomian decomposition method [19, 20], Adomian decomposition method [18], Homotopy perturbation method [21-29], Homotopy analysis method [30], Akabai-Ganji method [31-35] and Rajendran-Joy method [36]. In this paper, the Taylor series method is applied to solve the nonlinear model (equations (1)-(3)) for the immobilized enzyme reactions as per our assumptions considered for our enzyme kinetics for the three geometries, viz. planar, cylindrical and spherical. Then, the results are compared with the previous results of the same model solved by the respective authors using the modified Adomian decomposition method (MADM)[19]. Comparing these two methods with the numerical solutions, it is found that Taylor's series method yields the best approximations and converges at its fourth order. The analytical expression of the dimensionless substrate concentration in the immobilized enzyme reaction was obtained by solving (1-3) using Taylor's series method (Appendix A) as follows:

$$C(X) = l + \frac{(X-1)}{1!}B_i(1-l) + \frac{(X-1)^2}{2!}\left[\frac{\alpha^2 l}{1+\beta l} - (g-1)B_i(1-l)\right] + \frac{(X-1)^3}{3!}\left[g(g-1)B_i(1-l) - \frac{(g-1)\alpha^2 l}{1+\beta l} + \frac{\alpha^2 B_i(1-l)}{(1+\beta l)^2}\right] \tag{6}$$

where l values are obtained by applying the condition (2) in the derivative of the expression (6), as given in Appendix A, and substituting various possible values of the parameters α , β and B_i ,the l values have been collected as given in Tables S1, S2 and S3 corresponding to the planar, cylindrical and spherical geometries, respectively, and the general cubic expression in l is obtained and given below:

$$gB_i\beta^2 l^3 - \left[gB_i(\beta-2) - \alpha^2\right]\beta l^2 - \left[gB_i(2\beta-1) - \alpha^2 - \frac{\alpha^2 B_i}{g+1}\right]l - \left[g + \frac{\alpha^2}{(g+1)}\right]B_i = 0 \tag{7}$$

By applying the concentration expression (6) in (5), we obtain the effectiveness factor η as given below:

$$\eta = \frac{g(1+\beta)}{\alpha^2}B_i(1-l) \tag{8}$$

4. THE PREVIOUS ANALYTICAL RESULTS USING THE MODIFIED ADOMIAN DECOMPOSITION METHOD (KRISHNAN LAKSHMI NARAYANAN ET AL. [19])

Krishnan Lakshmi Narayanan et al. [19] derived the analytical expression for the dimensionless concentration profile by solving the nonlinear equation (1) by a modified Adomian

decomposition method. The approximate analytical expression obtained for the concentration profile is given below.

$$C(X) = 1 + \frac{1}{2g}\left\{\frac{\alpha^2}{(1+\beta)}\left[X^2 - \frac{2}{B_i} - 1\right] + \frac{\alpha^4}{(1+\beta)^3}\left[\frac{1}{20}(X^4 - 1) - \frac{1}{3}\left(\frac{1}{B_i} + \frac{1}{2}\right)\left(X^2 - \frac{2}{B_i} - 1\right) - \frac{1}{5B_i}\right]\right\} \quad (9)$$

The given geometry wise effectiveness factor values are obtained based on the solution expression (10) as follows: The general expression for the effectiveness factor has been derived using (9) in (5), as

$$\eta = 1 - \frac{2\alpha^2}{5(1+\beta)^2} \quad (10)$$

and this expression is common for all three geometries since the expression is independent of g and gives accurate results only for elliptical geometry. From Tables (7)-(9), we can infer that the numerical results are close to the analytical results obtained by this method only for elliptical geometry.

5. INFLUENCE OF PARTICLE SUBSTRATE GEOMETRIES

5.1 Planar Geometry

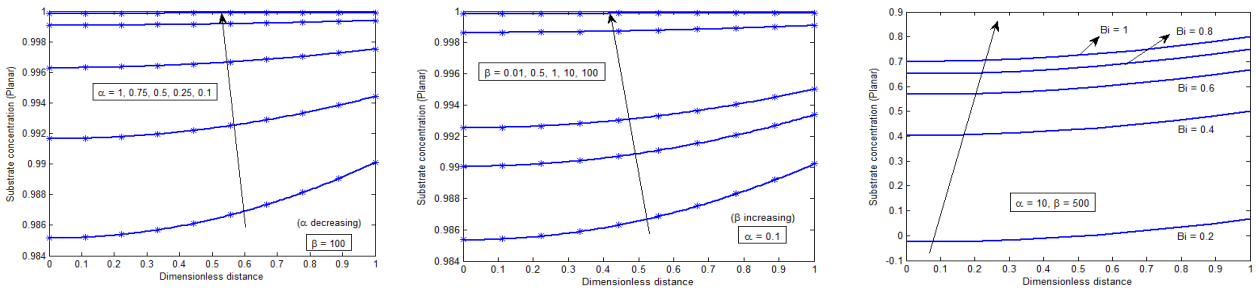

(a) **(b)** **(c)**

Figure 2. The dimensionless substrate concentration $C(X)$ versus the dimensionless distance X for the different values of the parameters α and β under the planar geometry, where the blue solid line represents the numerical results and (*****) represents the analytical results using Eq. (11). **(a)**Concentration variations while fixing that $B_i = 1$, $\beta = 100$ and varying the α values. **(b)** Concentration variations while fixing that $B_i = 1$, $\alpha = 0.1$ and varying the β values. **(c)** Concentration variations while fixing that $\alpha = 10, \beta = 500$ and varying the B_i values.

If g = 1, equation (6) yields the concentration of substrate *C* in the case of a planar particle substrate, such as

$$C(X) = l + \frac{(X-1)}{1!}B_i(1-l) + \frac{(X-1)^2}{2!}\left[\frac{\alpha^2 l}{1+\beta l}\right] + \frac{(X-1)^3}{3!}\left[\frac{\alpha^2 B_i(1-l)}{(1+\beta l)^2}\right] \quad (11)$$

where l is determined by solving the following equation (12) obtained by applying the condition (2) in the derivative of(11), as the result

$$-2B_i\beta^2 l^3 + (2B_i(\beta^2 - 2\beta) - 2\alpha^2\beta)l^2 + (2B_i(2\beta - 1) - 2\alpha^2 - \alpha^2 B_i)l + (\alpha^2 + 2)B_i = 0 \quad (12)$$

The value of l for various experimental values of other parameters is given in Table S1. Moreover, using (5), the overall effectiveness factor under this geometry is obtained as

$$\eta = \frac{(1+\beta)}{\alpha^2} B_i (1-l) \tag{13}$$

5.1.1. Discussion on the planar variations

The nonlinear reaction-diffusion equation (1) of our model along with the boundary conditions (2) and (3) has been solved for the dimensionless substrate concentration $C(X)$ by Taylor's series method, assuming that $C(1)=l$, a positive constant, and taking the Biot number $B_i = 0$ to 1 for all the geometries under consideration.The dimensionless substrate concentration obtained was given by equation (A.7), and the values of l were generated by solving equation (A.9) obtained by applying boundary condition (2) in (A.8).

Table 2. Comparison of the normalized steady state substrate concentration values of the Taylor series method and the modified Adomian decomposition method [19] with the numerical solution for various values of the parameters α, β and the corresponding values of l, taking the Biot number $B_i = 1$ with respect to the planar particle substrate.

X	Concentration $C(X)$									
	$\alpha = 0.1,\ \beta = 0.01$ and $l = 0.990243$					$\alpha = 0.5,\ \beta = 0.5$ and $l = 0.858494$				
	Numerical	TSM	MADM	Error in TSM	Error in MADM	Numerical	TSM	MADM	Error in TSM	Error in MADM
0	0.990000	0.985373	0.985209	0.467402	0.48392154	0.78	0.789184	0.761574	1.177483	2.3622982
0.1	0.990049	0.985421	0.985258	0.46744	0.48388293	0.780723	0.789851	0.762361	1.169295	2.35183981
0.2	0.990196	0.985567	0.985406	0.467517	0.48374794	0.782854	0.791864	0.764723	1.150959	2.31601768
0.3	0.990442	0.985810	0.985653	0.467631	0.4835206	0.786404	0.79524	0.768661	1.1237	2.25613729
0.4	0.990785	0.986150	0.985997	0.467774	0.48320438	0.79138	0.799997	0.774179	1.088823	2.17360579
0.5	0.991227	0.986588	0.986441	0.467943	0.48280224	0.797793	0.806151	0.781279	1.047689	2.06990725
0.6	0.991766	0.987124	0.986983	0.468133	0.4823166	0.80565	0.81372	0.789967	1.001689	1.94657638
0.7	0.992405	0.987757	0.987624	0.468338	0.4817493	0.814962	0.822722	0.80025	0.952218	1.80517162
0.8	0.993141	0.988488	0.988363	0.468554	0.48110169	0.825736	0.833173	0.812134	0.900653	1.64724875
0.9	0.993976	0.989316	0.989201	0.468775	0.48037453	0.837983	0.845091	0.825628	0.848328	1.47433579
1	0.994909	0.990243	0.990138	0.468998	0.47956808	0.85171	0.858494	0.840741	0.796515	1.28791012
	Average Error			0.468046	0.4823809	**Average Error**			1.023396	1.97191352

Here, for various values of the dimensionless parameters α and β, the dimensionlessconcentration profile has been preparedand clearly observed that the concentration levels obtained from both the analytical solution and the numerical solution have matched with each other for all the values of the parameters, as produced by Figures 2(a)-2(c), of which Figure 2(a) shows that the dimensionless substrate concentration level increases with respect to the increasing of β values while α is fixed at the least values 0.1 and 0.25, and similarly, it could be found as it moves so on.On the other hand, Figure 2(b) shows that the concentration level increases in accordance with the decreasing

of α values while β being fixed at the least value 0.01 and at a higher value 100 and similarly it could be found as moving so on for more higher values of β. Figure 2(c) shows the concentration variations while fixing $\alpha = 10, \beta = 500$ and varying B_i .

It is also found that the variation in the substrate concentration levels of the model has a high positive correlation with the corresponding variation in Biot numbers, as shown in Figure 2. Here, such variations have been shown for a particular set of values of the parameters, i.e., $\alpha = 10$ and $\beta = 500$. Additionally, observations, applying various sets of values of the parameters α and β, showed that for lower values of the parameters α and β, the substrate concentration levels are at higher values, whereas for higher values of the same parameters, the substrate concentration levels are at lower values under the planar geometry.

Furthermore, here, the dimensionless concentration profile has also been brought out using modified Adomian decomposition method [19], and the results of both the analytical methods have been compared to the numerical results obtained using MATLAB software and produced all such comparisons of the variations between the concentration levels for such sets of values of the parameters α and β andtabulated as Table 2.From this comparison, it is clearly observed that concentration levels under the Taylor series method results are always much better than those of modified Adomian decomposition method.

The overall effectiveness factor, η corresponding to this geometry, is given in equation (13) obtained from (5) for g = 1, and the values obtained, for various values of the Thiele modulus α and the dimensionless concentration under Michaelis–Menten kinetics, β, are tabulated in Table 7.Figure S1 (a) shows the flow of the effectiveness factor η against the Thiele modulus α, and Figure S1 (b) shows the flow of the effectiveness factor η against the Michaelis–Menten constant β under this geometry. By the observation, it is inferred that a decreasing trend of the Thiele modulus improves the effectiveness factor levels, whereas the increasing trend of the values of the Michaelis–Menten constant improves the effectiveness factor levels. Similarly, the overall effectiveness factor values have been found using the modified Adomian decomposition method concentration results based on its corresponding effectiveness factor [19] given by equation (13), and both the analytical results of the effectiveness factor η have been compared with the numerical results in the same table. By comparing the results, it is realized that the Taylor series method results better fit the numerical results.Moreover, there is a drawback that the effectiveness factor formula of the modified Adomian decomposition method is independent of the particle substrate shape facto, which causes controversy in showing the variations in the results among the different geometries.

5.2. Cylindrical Geometry

If g = 2, equation (6) yields the concentration of the substrate, *C*, in the case of a cylindrical shape particle substrate, such as

$$C(X) = l + \frac{(X-1)}{1!}B_i(1-l) + \frac{(X-1)^2}{2!}\left[\frac{\alpha^2 l}{1+\beta l} - B_i(1-l)\right] + \frac{(X-1)^3}{3!}\left[2B_i(1-l) - \frac{\alpha^2 l}{1+\beta l} + \frac{\alpha^2 B_i(1-l)}{(1+\beta l)^2}\right] \quad (14)$$

where *l* is determined by solving equation (17), which is obtained by applying condition (2).

$$-6B_i\beta^2 l^3+(6B_i(\beta^2-2\beta)-3\alpha^2\beta)l^2+(6B_i(2\beta-1)-3\alpha^2-\alpha^2B_i)l+(\alpha^2+6)B_i=0 \quad (15)$$

Moreover, using (7), the overall effectiveness factor under this geometry is obtained as

$$\eta=\frac{2(1+\beta)}{\alpha^2}B_i(1-l) \quad (16)$$

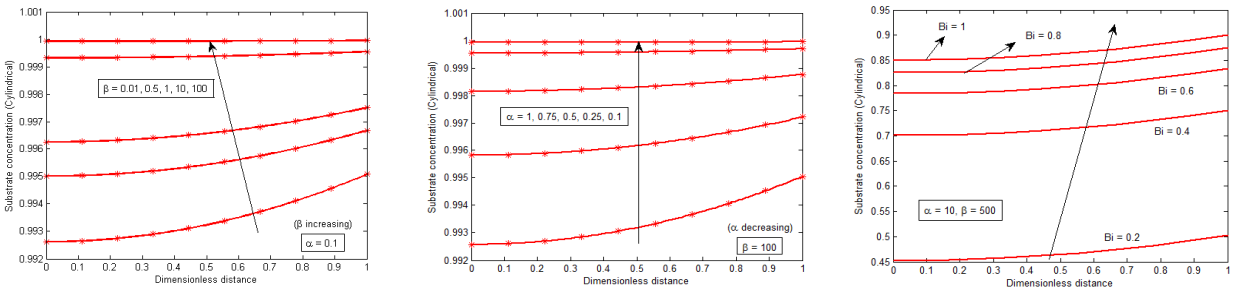

(a) **(b)** **(c)**

Figure 3. The dimensionless substrate concentration $C(X)$ versus the dimensionless distance X for the different values of the parameters α and β under the cylindrical geometry, where the red solid line represents the numerical results and (*****) represents the analytical results using Eq. (14). **(a)** Concentration variations while fixing that $\alpha=0.1$, $B_i=1$ and varying the β values. **(b)**Concentration variations while fixing that $\beta=100$, $B_i=1$ and varying the α values. **(c)** Concentration variations while fixing that $\alpha=10,\beta=500$ and varying the B_i values.

5.2.1. Discussion on the cylindrical variations

Here, for various values of the dimensionless parameters α and β, the dimensionless concentration profile has been preparedand clearly observed that the concentration levels obtained from both the analytical solution and the numerical solution have matched with each other for all the values of the parameters, as produced by Figures 3(a)-3(c), of which Figure 3(a) shows that the dimensionless substrate concentration level increases with respect to the increasing of β values while α is fixed at the least values 0.1 and 0.75, and similarly, it could be found as it moves so on for various dimensionless values of α .On the other hand, Figure 3(b) shows that the concentration level increases in accordance with the decreasing of α values while β being fixed at the least value 0.01 and at a higher value 100 and similarly it could be found as moving so on for higher values of β. Figure 3(c) shows the concentration variations while fixing $\alpha=10,\beta=500$ and varying. B_i .

Furthermore, here, the dimensionless concentration profile has also been brought out using modified Adomian decomposition method [19], and the results of both the analytical methods have been compared to the numerical results obtained using MATLAB software and produced all such comparisons of the variations between the concentration levels for such sets of values of the parameters α and β and tabulated as Table 4.From this comparison, it is clearly observed that concentration levels under the Taylor series method results are always much better than those of modified Adomian decomposition method. The overall effectiveness factor, η corresponding to this geometry, is given in equation (16) obtained from (5) for various values of the Thiele modulus α and

the dimensionless concentration under the Michaelis–Menten kinetics, β which are tabulated in Table S2.

Figure S2(a) shows the flow of the effectiveness factor η against the Thiele modulus α, and Figure S2(b) shows the flow of the effectiveness factor η against the Michaelis–Menten constant β under this geometry.Then, by observation, it is inferred that a decreasing trend of the Thiele modulus improves the effectiveness factor levels, whereas the increasing trend of the values of the Michaelis–Menten constant improves the effectiveness factor levels. Similarly, the overall effectiveness factor values have been found using the modified Adomian decomposition method concentration results based on its corresponding effectiveness factor [19] given by equation (16), and both the analytical results of the effectiveness factor η have been compared with the numerical results in the same table. By comparing the results, it is realized that the Taylor series method results better fit the numerical results.Moreover, according to the same drawback that the effectiveness factor formula of the modified Adomian decomposition method is independent of the particle substrate shape factor; it may cause improper variations in the results among the different geometries.

Table 4. Comparison of the normalized steady state substrate concentration values of the Taylor series method and the modified Adomian decomposition method [19] with the numerical solution for various values of the parameters α, β and the corresponding values of l, taking the Biot number $B_i = 1$ with respect to the cylindrical particle substrate.

X	Concentration $C(X)$									
	$\alpha = 0.1,\ \beta = 0.01$ and $l = 0.995082$					$\alpha = 0.5,\ \beta = 0.5$ and $l = 0.922591$				
	Numerical	TSM	MADM	Error in TSM	Error in MADM	Numerical	TSM	MADM	Error in TSM	Error in MADM
0	0.99	0.992626	0.992605	0.265268	0.26308973	0.88	0.884389	0.880787	0.498784	0.08943603
0.1	0.990025	0.992651	0.992629	0.265165	0.26300884	0.880394	0.884762	0.881181	0.49623	0.08938828
0.2	0.990101	0.992724	0.992703	0.264951	0.26283706	0.881551	0.885885	0.882361	0.491691	0.09195175
0.3	0.990226	0.992847	0.992826	0.264626	0.26257159	0.883475	0.887764	0.884331	0.485452	0.09678918
0.4	0.990402	0.993018	0.992999	0.26419	0.26220997	0.886171	0.890405	0.887089	0.47781	0.10361648
0.5	0.990627	0.993239	0.99322	0.263643	0.26175006	0.889641	0.893814	0.890639	0.469062	0.11220451
0.6	0.990903	0.993509	0.993491	0.262984	0.26119003	0.89389	0.897997	0.894984	0.459508	0.12238016
0.7	0.991229	0.993829	0.993812	0.262215	0.26052839	0.89892	0.90296	0.900125	0.449448	0.1340267
0.8	0.991606	0.994197	0.994181	0.261335	0.25976397	0.904736	0.90871	0.906067	0.439178	0.14708341
0.9	0.992032	0.994615	0.994601	0.260344	0.25889594	0.911342	0.915251	0.912814	0.428988	0.16154446
1	0.992509	0.995082	0.995069	0.259242	0.25792378	0.91874	0.922591	0.92037	0.419161	0.17745721
Average Error				0.263087	0.26125176	**Average Error**			0.465028	0.12053438

5.3. Spherical Geometry

If g = 3, equation (6) yields the concentration of the substrate$C$ in the case of a spherically shaped particle substrate, such as

$$C(X) = l + \frac{(X-1)}{1!}B_i(1-l) + \frac{(X-1)^2}{2!}\left[\frac{\alpha^2 l}{1+\beta l} - 2B_i(1-l)\right] + \frac{(X-1)^3}{3!}\left[6B_i(1-l) - \frac{2\alpha^2 l}{1+\beta l} + \frac{\alpha^2 B_i(1-l)}{(1+\beta l)^2}\right] \quad (17)$$

where l is determined by solving the following equation (20) obtained by applying the condition (2) in the derivative of(19), as the result

$$-12B_i\,\beta^2 l^3+(12B_i\,(\beta^2-2\beta)-4\alpha^2\beta)l^2+(12B_i\,(2\beta-1)-4\alpha^2-\alpha^2B_i)l+(\alpha^2+12)B_i=0 \quad (18)$$

Moreover, using (7), the overall effectiveness factor under this geometry is obtained as

$$\eta=\frac{3(1+\beta)}{\alpha^2}B_i(1-l) \quad (19)$$

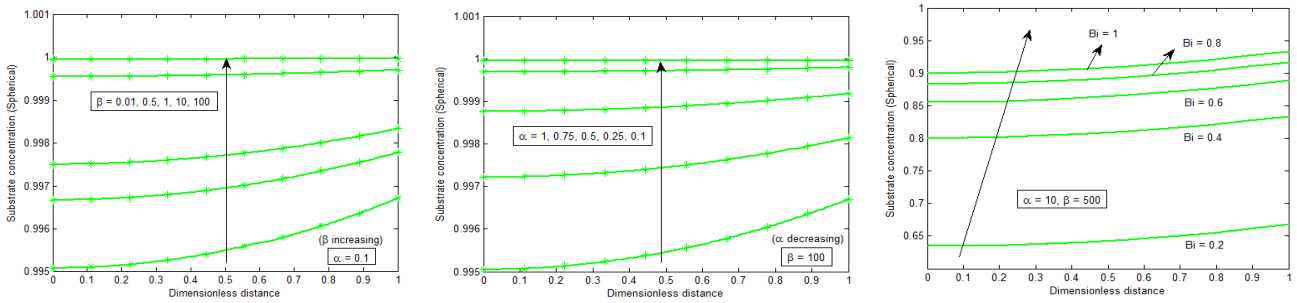

(a) **(b)** **(c)**

Figure 4. The dimensionless substrate concentration $C(X)$ versus the dimensionless distance X for the different values of the parameters α and β under spherical geometry, where the green solid line represents the numerical results and (*****) represents the analytical results using Eq. (17). **(a)**Concentration variations while fixing that $\alpha=0.1, B_i=1$ and varying the β values. **(b)** Concentration variations while fixing that $\beta=100$, $B_i=1$ and varying the α values. **(c)** Concentration variations while fixing that $\alpha=10, \beta=500$ and varying the B_i values.

5.3.1. Discussion on the spherical variations

Here, for various values of the dimensionless parameters α and β, the dimension less concentration profile has been preparedand clearly observed that the concentration levels obtained from both the analytical solution and the numerical solution have matched with each other for all the values of the parameters, as produced by Figures 4(a)-4(c), of which Figure 4(a) shows that the dimensionless substrate concentration level increases with respect to the increasing of β values while α is fixed at the least values 0.1 and 1.0, and similarly, it could be found as it moves so on for various dimensionless values of α .On the other hand, Figure 4(b) shows that the concentration level increases in accordance with the decreasing of α values while β being fixed at the least value 0.01 and at a higher value 100 and similarly it could be found as moving so on for more higher values of β. Figure 3(c) shows the concentration variations while fixing $\alpha=10, \beta=500$ and varying B_i . Furthermore, the dimensionless concentration profile has also been brought out using modified Adomian decomposition method [19], and the results of both the analytical methods have been compared to the numerical results obtained using MATLAB software and produced all such comparisons of the variations between the concentration levels for such sets of values of the parameters α and β and tabulated as Table 6.From this comparison, it is clearly observed that concentration levels under the Taylor series method results are always much better than those of modified Adomian decomposition method.

Figure 6(a) shows the flow of the effectiveness factor η against the Thiele modulus α, and Figure 6(b) shows the flow of the effectiveness factor η against the Michaelis–Menten constant β under this geometry.Then, by observation, it is inferred that a decreasing trend of the Thiele modulus improves the effectiveness factor levels, whereas the increasing trend of the values of the Michaelis–Menten constant improves the effectiveness factor levels. Similarly, the overall effectiveness factor values have been found using the modified Adomian decomposition method concentration results based on its corresponding effectiveness factor [19] given by equation (12), and both the analytical results of the effectiveness factor η have been compared with the numerical results in the same table. By comparing the results, it is realized that the Taylor series method results better fit the numerical results.Moreover, according to the same drawback that the effectiveness factor formula of the modified Adomian decomposition method is independent of the particle substrate shape factor; it may cause improper variations in the results among the different geometries.

Figures 5(a)-5(c) show the variations in the dimensionless concentration levels for the three geometries for different sets of parameter values, taking the Biot number as $B_i = 1$. Figure 6 shows the comparative variation in the geometry wise concentration levels among the three geometries for a particular set of parameter values. Figures 10(a) and 10(b) show the geometry wise comparative display of the variations of the overall effectiveness factor values against the Thiele modulus α and against the Michaelis–Menten constant β, respectively.

Table 6. Comparison of the normalized steady state substrate concentration values of the Taylor series method and the modified Adomian decomposition method [19] with the numerical solution for various values of the parameters α, β and the corresponding values of l, taking the Biot number $B_i = 1$ with respect to spherical particle substrate.

X	Concentration $C(X)$									
	$\alpha = 0.1,\ \beta = 0.01$ and $l = 0.996713$					$\alpha = 0.5,\ \beta = 0.5$ and $l = 0.946954$				
	Numerical	TSM	MADM	Error in TSM	Error in MADM	Numerical	TSM	MADM	Error in TSM	Error in MADM
0	1	0.995071	0.99507	0.49294	0.49302744	0.92	0.920687	0.920525	0.074652	0.05703167
0.1	1.000016	0.995087	0.995086	0.492892	0.49298293	0.920265	0.920945	0.920787	0.073838	0.05671653
0.2	1.000064	0.995136	0.995135	0.49275	0.49283952	0.921052	0.921721	0.921574	0.072595	0.05670048
0.3	1.000144	0.995218	0.995218	0.492514	0.49259809	0.922363	0.923018	0.922887	0.071055	0.05684124
0.4	1.000256	0.995333	0.995332	0.492181	0.49225932	0.924199	0.92484	0.924726	0.069352	0.05703672
0.5	1.000401	0.995481	0.99548	0.491753	0.49182374	0.926563	0.927189	0.927093	0.067617	0.05722531
0.6	1.000577	0.995662	0.995661	0.491229	0.49129169	0.929456	0.930069	0.929989	0.065981	0.05738582
0.7	1.000785	0.995875	0.995875	0.490608	0.49066335	0.93288	0.933482	0.933417	0.064574	0.0575371
0.8	1.001025	0.996121	0.996121	0.48989	0.4899387	0.936837	0.937432	0.937378	0.063523	0.05773732
0.9	1.001298	0.996401	0.9964	0.489074	0.48911756	0.941329	0.941922	0.941876	0.062951	0.05808291
1	1.001602	0.996713	0.996713	0.488161	0.48819958	0.946358	0.946954	0.946914	0.062978	0.0587072
	Average Error			0.491272	0.49134018	**Average Error**			0.068101	0.05736385

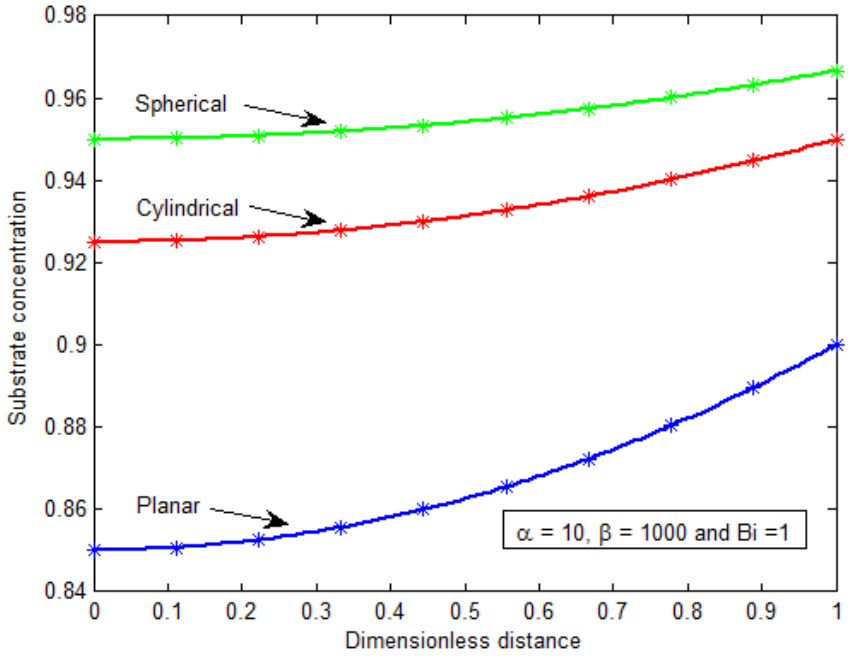

Figure 5. The comparison of the variations among the three geometrical outputs of the dimensionless substrate concentration $C(X)$ versus the dimensionless distance X at a position for which the values of the parameters taken are $\alpha = 10$ and $\beta = 1000$ for $B_i = 1$, in which the blue solid line with (*) represents the solutions under planar geometry, the red solid line with (*) represents the solutions under cylindrical geometry and the green solid line with (*) represents the solutions under spherical geometry.

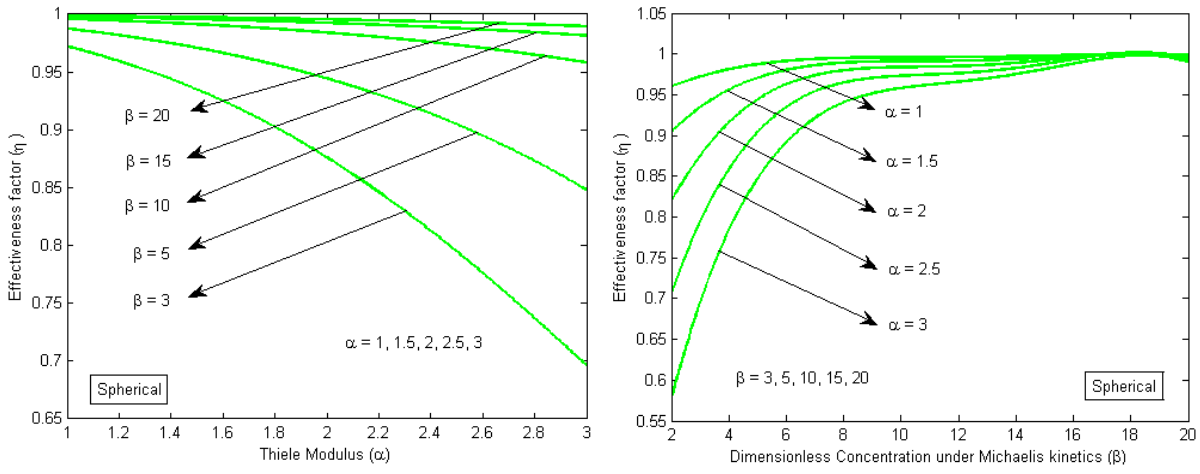

(a) **(b)**

Figure 6. When $B_i = 1$. **(a)** The effectiveness factor η against the Thiele modulus α. **(b)**The effectiveness factor η against the dimensionless Michaelis–Menten constant β.

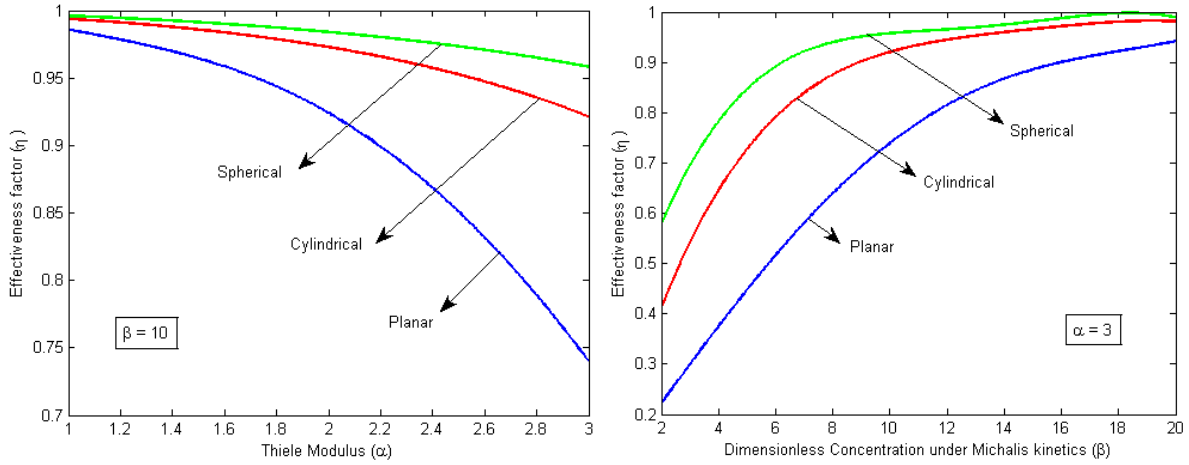

(a) **(b)**

Figure 7. (a) Geometry of the effectiveness factor η against the Thiele modulus α. (b) Geometry wise effectiveness factor η against the dimensionless Michaelis–Menten constant β.

Table 7. Comparison of the effectiveness factor variations under Taylor series method and modified Adomian decomposition method [19] analytical results with numerical results by planar shape particle substrate for various values of the Theile Modulus α and various values of β, with $B_i = 1$.

	$\alpha=1$					$\alpha=2$					$\alpha=3$				
β	Numerical η	TSM η	MADM η	Error by TSM	Error by MADM	Numerical η	TSM η	MADM η	Error by TSM	Error by MADM	Numerical η	TSM η	MADM η	Error by TSM	Error by MADM
	Ef					Ef					Ef				
1	0.8477	0.8392	0.9000	1.0084	6.1671	0.5160	0.5077	0.6000	1.9803	15.8301	0.2907	0.2873	0.1000	1.1639	65.596
10	1.0159	0.9942	0.9967	2.133163	1.8899	0.9691	0.9732	0.9868	0.4245	1.8240	0.9255	0.9214	0.9702	0.4361	4.8388
25	1.0008	0.9990	0.9994	0.1819	0.1383	0.9915	0.9957	0.9976	0.4196	0.6176	0.9886	0.9890	0.9947	0.0403	0.6167
50	1.0018	0.9997	0.9998	0.2077	0.1933	1.0224	0.9989	0.9994	2.2970	2.2532	1.0003	0.9974	0.9986	0.2866	0.1675
75	1.0054	0.9999	0.9999	0.5473	0.5399	0.9902	0.9995	0.9997	0.9363	0.9574	1.0158	0.9989	0.9994	1.6676	1.6183
100	1.0121	0.9999	1.0000	1.2055	1.1995	1.0021	0.9997	0.9998	0.2318	0.2224	0.9899	0.9994	0.9996	0.9591	0.9857
		Average		0.8806	1.6880		**Average**		1.0483	3.6175		**Average**		0.7589	12.304

Table 8. Comparison of the effectiveness factor variations under Taylor series method and modified Adomian decomposition method [19] analytical results with numerical results by cylindrical shape particle substrate for various values of the Theile Modulus α and various values of β, with $B_i = 1$.

	$\alpha=1$					$\alpha=2$					$\alpha=3$				
β	Numerical η	TSM η	MADM η	Error by TSM	Error by MADM	Numerical η	TSM η	MADM η	Error by TSM	Error by MADM	Numerical η	TSM η	MADM η	Error by TSM	Error by MADM
	Ef					Ef					Ef				
1	0.7152	0.6749	0.9000	5.6309	25.839	0.3030	0.2929	0.6000	3.3356	98.020	0.1529	0.1460	0.1000	4.4738	34.593

10	0.9927	0.9863	0.9967	0.6449	0.4029	0.9032	0.9243	0.9868	2.3433	9.2589	0.7277	0.7407	0.9702	1.7860	33.329
25	0.9884	0.9977	0.9994	0.9381	1.1137	0.9904	0.9891	0.9976	0.1326	0.7258	0.9922	0.9670	0.9947	2.5341	0.2534
50	0.9997	0.9994	0.9998	0.0259	0.0192	0.9950	0.9974	0.9994	0.2477	0.4426	0.9988	0.9933	0.9986	0.5503	0.0225
75	1.0032	0.9997	0.9999	0.3454	0.3228	0.9882	0.9989	0.9997	1.0806	1.1652	0.9970	0.9972	0.9994	0.0221	0.2357
100	1.0099	0.9999	1.0000	0.9922	0.9862	1.0101	0.9994	0.9998	1.0634	1.0165	0.9879	0.9985	0.9996	1.0788	1.1940
		Average		1.4296	4.7806		**Average**		1.3672	18.438		**Average**		1.7409	11.605

Table 9. Comparison of the effectiveness factor variations under Taylor series method and modified Adomian decomposition method [19] analytical results with numerical results by spherical shape particle substrate for various values of the Theile Modulus α and various values of β, with $B_i = 1$.

	$\alpha=1$					$\alpha=2$					$\alpha=3$				
β	Numerical η	TSM η	MADM η	Error by TSM	Error by MAD	Numerical η	TSM η	MADM η	Error by TSM	Error by MADM	Numerical η	TSM η	MADM η	Error by TSM	Error by MADM
1	0.8954	0.8973	0.9000	0.2191	0.5160	0.6543	0.6415	0.6000	1.9553	8.2989	0.4047	0.4056	0.1000	0.2399	75.288
10	0.9917	0.9965	0.9967	0.4768	0.4996	0.9808	0.9844	0.9868	0.3676	0.6076	0.9775	0.9586	0.9702	1.9296	0.7378
25	0.9990	0.9993	0.9994	0.0320	0.0392	1.0154	0.9974	0.9976	1.7765	1.7522	0.9913	0.9937	0.9947	0.2334	0.3367
50	1.0102	0.9999	0.9998	1.0283	1.0292	0.9951	0.9994	0.9994	0.4236	0.4263	0.9870	0.9985	0.9986	1.1572	1.1729
75	1.0036	1.0000	0.9999	0.3587	0.3664	1.0037	0.9997	0.9997	0.3953	0.3953	1.0140	0.9993	0.9994	1.4458	1.4406
100	0.9700	0.9999	1.0000	3.0822	3.0884	1.0004	0.9998	0.9998	0.0538	0.0519	1.0105	0.9996	0.9996	1.0791	1.0775
		Average		0.8662	0.9232		**Average**		0.8287	1.9220		**Average**		1.0142	13.342

6. CONCLUSION

In this work, an approximate analytical solution for a mathematical model for the dimensionless substrate concentrations caused by the immobilization of the enzymes for the case with external mass transfer resistance, taking the Biot number $B_i = 1$, upon all three geometries viz. planar, cylindrical and spherical were obtained by using Taylor's series method. These results have also been compared with the results produced by another analytical technique, namely, the modified Adomian decomposition method (MADM. Similarly, the overall effectiveness factor variations caused by such concentration levels have also been found by using these two analytical methods, and consequently, on by comparing these analytical results with the numerical results of the model obtained with the help of MATLAB software, it has been realized that the Taylor series method yields better results, and comparison tables and graphs have been produced for various values of the parameters. It was clearly observed that Taylor's series method is straightforward with a simple solution process and yields accurate results much closer to the numerical solutions at its third-order itself. This procedure can be extended without any difficulty to other boundary value problems in the physical, chemical and biosciences.

Appendix A:

ANALYTICAL SOLUTION OF NONLINEAR EQUATIONS (1)-(3) USING THE TAYLOR SERIES METHOD.

Equation (1) can be rewritten as

$$[XC''(X)+(g-1)C'(X)](1+\beta C(X))-\alpha^2 XC(X)=0 \quad \text{(A.1)}$$

In this paper, we consider a simple approach by Taylor's series method for solving for the dimensionless substrate concentration, *C*.

For*X* = 1, we have

$$[C''(1)+(g-1)C'(1)](1+\beta C(1))-\alpha^2 C(1)=0 \quad \text{(A.2)}$$

Applying boundary condition (3) in (A.2), for X = 1, we obtain

$$[C''(1)+(g-1)B_i(1-C(1))](1+\beta C(1))-\alpha^2 C(1)=0 \quad \text{(A.3)}$$

Assuming that $C(1) = l$,we will have that

$$[C''(1)+(g-1)B_i(1-l)](1+\beta l)-\alpha^2 l=0 \quad \text{(A.4)}$$

from which we obtain

$$C''(1)=\frac{\alpha^2 l}{1+\beta l}-(g-1)B_i(1-l) \quad \text{(A.5)}$$

Now, as in the above case, applying boundary condition (3) and our assumption in the derivative of (A.1), for $X = 1$, we obtain

$$C'''(1)=g(g-1)B_i(1-l)-\frac{(g-1)\alpha^2 l}{1+\beta l}+\frac{\alpha^2 B_i(1-l)}{(1+\beta l)^2} \quad \text{(A.6)}$$

Then, by using boundary condition (3) and equations (A.5), and (A.6)along with our assumption, in Taylor's series about $X = 1$,we obtain

$$C(X)=l+\frac{(X-1)}{1!}B_i(1-l)+\frac{(X-1)^2}{2!}\left[\frac{\alpha^2 l}{1+\beta l}-(g-1)B_i(1-l)\right]+\frac{(X-1)^3}{3!}\left[g(g-1)B_i(1-l)-\frac{(g-1)\alpha^2 l}{1+\beta l}+\frac{\alpha^2 B_i(1-l)}{(1+\beta l)^2}\right] \quad \text{(A.7)}$$

Differentiating this with respect to *X*, we obtain

$$C'(X)=B_i(1-l)+(X-1)\left[\frac{\alpha^2 l}{1+\beta l}-(g-1)B_i(1-l)\right]+\frac{(X-1)^2}{2}\left[g(g-1)B_i(1-l)-\frac{(g-1)\alpha^2 l}{1+\beta l}+\frac{\alpha^2 B_i(1-l)}{(1+\beta l)^2}\right] \quad \text{(A.8)}$$

Now, by applying condition (2) in (A.8), we obtain

$$gB_i\beta^2 l^3-\left[gB_i(\beta-2)-\alpha^2\right]\beta l^2-\left[gB_i(2\beta-1)-\alpha^2-\alpha^2 B_i\right]l-\left[g+\frac{\alpha^2}{(g+1)}\right]B_i=0 \quad \text{(A.9)}$$

Solving equation (A.9) for *l* and substituting that value in (A.7), we will obtain the dimensionless substrate concentration *C* for the case with external mass transfer resistance.

Appendix B: MATLAB Coding

```
function pdex4
m=0;
x=linspace(0,1);
t=linspace(0,1000);
sol=pdepe(m,@pdex4pde,@pdex4ic,@pdex4bc,x,t);
u1=sol(:,:,1);
%-------------------------------------------------------------
figure
plot(x,u1(end,:))
title('u1(x,t)')
xlabel('Distance x')
ylabel('u1(x,1)')
```

```
function[c,f,s]=pdex4pde(x,t,u,DuDx)
c=1;
f=1.*DuDx;
a=0.1; b=0.5;
F=-((a^2*u(1))/(1+b*u(1)));
s=F;
%-------------------------------------------------------------
function u0=pdex4ic(x)
u0=[0];
%-------------------------------------------------------------
function[pl,ql,pr,qr]=pdex4bc(~,~,~,ur,t)
B=1;
pl=[0];
ql=[1];
pr=[-B*(1-ur(1))];
qr=[1];
```

DECLARATIONS

FUNDING
No funding was received to assist with the preparation of this manuscript.

CONFLICTS OF INTEREST/COMPETING INTERESTS
The authors declare that there are no conflicts of interest.

AVAILABILITY OF DATA AND MATERIAL
Data sharing is not applicable to this article, as no datasets were generated or analysed during the current study.

ACKNOWLEDGEMENT
The Authors are very much grateful to the management, SRM Institute of Science and Technology, Kattankulathur, for their continuous support and encouragement.

SUPPLEMENTARY MATERIAL OF THE MANUSCRIPT

Table S1. Numerical values of the parameter *l* for various values of the parameters α, β and for a fixed value of Biot number $B_i = 1$ in the case of a planar shape particle substrate.

β \ α	0.1	0.25	0.5	0.75	1	5	10
0.01	0.990243	0.943331	0.819126	0.695743	0.600483	0.349972	0.337026
0.1	0.99102	0.947292	0.82737	0.70326	0.605052	0.344151	0.330799
0.5	0.99338	0.96003	0.858494	0.736706	0.628921	0.322929	0.307881
1	0.995019	0.96948	0.886506	0.774602	0.662536	0.303488	0.286489
10	0.99909	0.994323	0.977345	0.949241	0.910337	0.221269	0.17362
100	0.999901	0.999381	0.997525	0.994431	0.990100	0.753801	0.174847
500	0.99998	0.999875	0.999501	0.998877	0.998004	0.950108	0.800560
1000	0.99999	0.999938	0.999750	0.999438	0.999001	0.975026	0.900117

Table S2. Numerical values of the parameter l for various values of the parameter α, β and for a fixed value of Biot number $B_i = 1$ in the case of a cylindrical particle substrate.

β \ α	0.1	0.25	0.5	0.75	1	5	10
0.01	0.995082	0.970274	0.893638	0.796524	0.701049	0.292084	0.260639
0.1	0.995479	0.972539	0.900259	0.805846	0.710423	0.288906	0.256783
0.5	0.996677	0.979549	0.922591	0.840895	0.749497	0.277368	0.242275
1	0.997504	0.984538	0.940093	0.872373	0.790207	0.267097	0.228355
10	0.999545	0.99716	0.988652	0.974513	0.954808	0.282075	0.154000
100	0.999950	0.999691	0.998762	0.997215	0.99505	0.876476	0.512544
500	0.99999	0.999938	0.99975	0.999439	0.999002	0.975052	0.90023
1000	0.999995	0.999969	0.999875	0.999719	0.999500	0.987513	0.950053

Table S3. Numerical values of the parameter l for various values of the parameter α, β and for a fixed value of Biot number $B_i = 1$ in the case of a spherically shaped particle substrate.

β \ α	0.1	0.25	0.5	0.75	1	5	10
0.01	0.996713	0.979887	0.925143	0.849091	0.765867	0.269887	0.218457
0.1	0.99698	0.981460	0.93029	0.857569	0.776026	0.268304	0.21591
0.5	0.997782	0.986271	0.946954	0.887294	0.81481	0.262933	0.206178
1	0.998335	0.989651	0.959417	0.911712	0.850443	0.259066	0.196667
10	0.999697	0.998106	0.992431	0.982988	0.969804	0.389796	0.149009
100	0.999967	0.999794	0.999175	0.998144	0.99670	0.917585	0.67214
500	0.999993	0.999958	0.999834	0.999626	0.999335	0.983367	0.933478
1000	0.999997	0.999979	0.999917	0.999813	0.999667	0.991675	0.966701

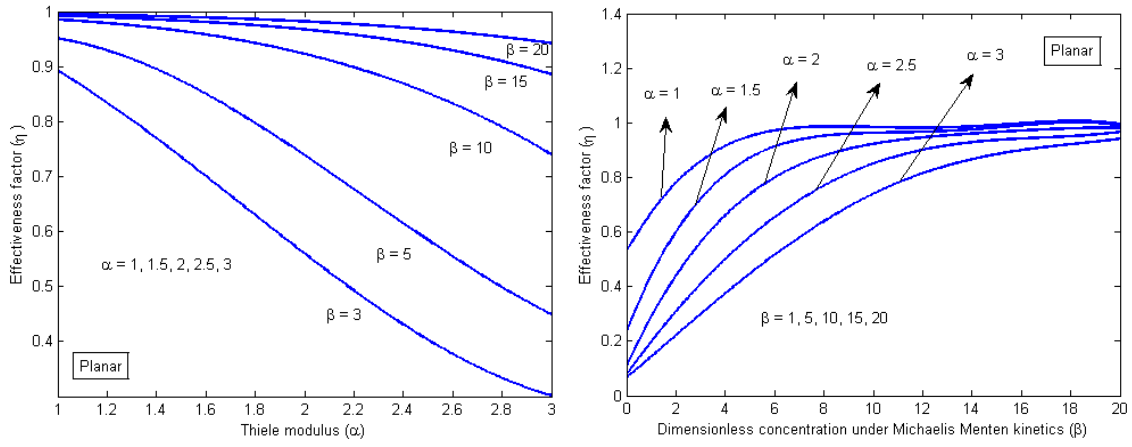

(a) **(b)**

Figure S1. (a) The effectiveness factor η against the Thiele modulus α. **(b)** The effectiveness factor η against the dimensionless Michaelis–Menten constant β.

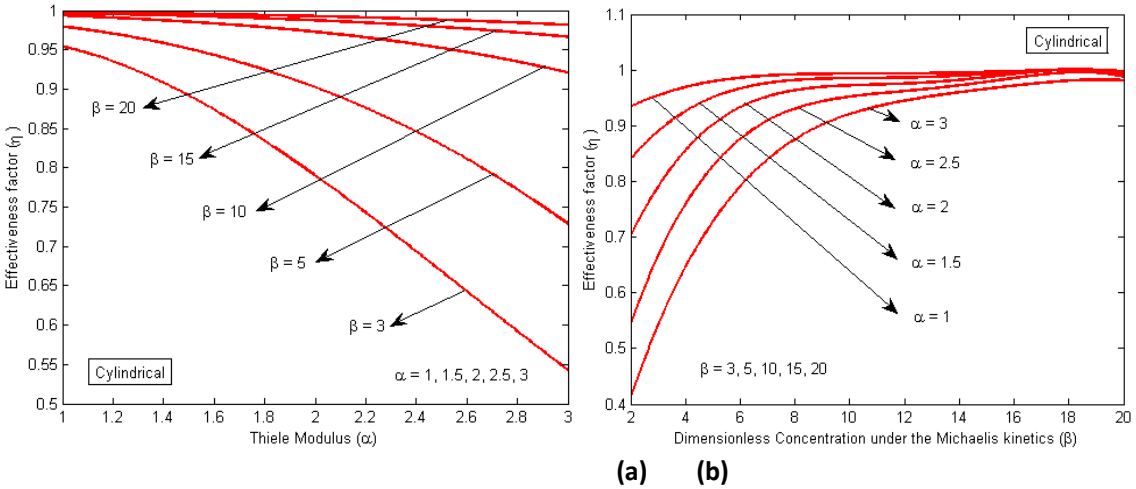

Figure S2.(a) The effectiveness factor η against the Thiele modulus α. **(b)**The effectiveness factor η against the dimensionless Michaelis–Menten constant β.

References

1. D.J. Fink, T.Y. Na and J.S. Schultz, *Biotechnol. Bioeng*., 15 (1973) 879.
2. A. Kheirolomoom, S. Katoh, E. Sada and K. Yoshida, *Biotechnol. Bioeng*., 37 (1991) 809.
3. S.A. Mireshghi, A. Kheirolomoom and F. Khorasheh, *Sci. Iran*., 3(3) (2001) 189.
4. J.Y. Houng, H. Yu, K.C. Chen and C. Tiu, *Biotechnol. Bioeng.*, 41 (1993) 451.
5. L. Goldstein, *Meth. Enzymol.*, 44 (1976) 397.
6. T. Kobayashi and K.J. Laidler, *Biochim. Biophys. Acta.*, 302 (1973) 1.
7. I.H. Segel, Enzyme Kinetics, Wiley, New York (1993)227.
8. R. Senthamarai and T.N. Saibavani, *IOP Conf. Series: J. Phys.*, 1000 (2018) 012146.
9. M. Matinfar and M. Ghasemi, *Int. J. Numer. Methods for Heat Fluid Flow*, 23 (2013) 520.
10. E. Miletics, G. Molnarka,*J. Comp. Methods. Sci. Eng.*, 4 (2004) 105.
11. J.H. He and F.Y. Ji, *J. Math. Chem.*, 57(8) (2019) 1932.
12. R.U. Rani, L. Rajendran and M.E. Lyons, *J. Electroanal. Chem*.886 (2021) 115103.
13. R.U. Rani, and L. Rajendran, *Chem. Phys. Lett.*, 754 (2020) 137573.
14. S. Vinolyn Sylvia, R. Joy Salomi, L. Rajendran and M. Abukhaled, *J. Math. Chem.*, 59 (5) (2021) 1332.
15. L.C. Mary, R.U. Rani, A. Meena and L. Rajendran, *Int. J. Electrochem. Sci.*, 16 (2021) 151037.
16. P. Rentrop, *Num. Math.*, 31 (1978) 359.
17. R. Umadevi, M. Chitra Devi, K. Venugopal, L. Rajendran and M.E.G. Lyons, *Int. J. Electrochem. Sci.*, 17 (2022) 220560.
18. M.L.C. Mary, M. Chitra Devi, A. Meena, L. Rajendran and M. Abukhaled, *J. Math. Comput. Sci.* 11 (2021) 8354.
19. K. L. Narayanan, V. Meena, L. Rajendran, J. Gao and S.P. Subbiah, *Appl. And,Comput. Math.* 6 (3) (2017) 143.
20. R. Rach, J. S. Duan and A. M. Wazwaz, *Chem. Eng. Comm.*, 202 (8) (2015) 1081.
21. G. Sivashankari and R. Senthamarai, *AIP Conf. Proc.*, 2277 (2020) 210004.
22. M. Sivakumar and R. Senthamarai, *AIP Conf. Proc.*, 2277 (2020) 130009.
23. M. Nivethitha and R. Senthamarai, *AIP Conf. Proc.*, 2277 (2020) 210005.
24. T. Vijayalakshmi and R. Senthamarai, *Int. J. of Adv. Sci. and Technol.*, 29(6) (2020) 2853.
25. G. Suganya and R. Senthamarai, *AIMS Mathematics*, 7(7) (2022) 13053.

26. R. Umadevi, K. Venugopal, P. Jeyabarathi, L. Rajendran and M. Abukhaled, *PJM*, 11 (2022) 316.
27. B. Manimegalai, M.E.G. Lyons and L. Rajendran, *J. Electroanal. Chem.* 902 (2021) 115775.
28. R. Joy Salomi, S. Vinolyn Sylvia, L. Rajendran and M.E.G. Lyons, *J. Electroanal. Chem.* 895 (2021) 115421.
29. B. Manimegalai, L. Rajendran and M.E.G. Lyons, *Int. J. Electrochem. Sci*., 16 (2021)210946.
30. R. Swaminathan, R. Saravanakumar, K. Venugopal and L. Rajendran, *Int. J. Electrochem. Sci.*, 16 (2021)210644.
31. S. SalaiSivasundari, R. Usha Rani, M.E.G. Lyons and L. Rajendran, *Int. J. Electrochem. Sci.*, 17 (2022) 220447.
32. R. Shanthi, M. Chitra Devi, M. Abukhaled, M.E.G. Lyons and L. Rajendran, *Int. J. Electrochem. Sci.*, 17 (2022) 220349.
33. S. Padma, P. Jeyabarathi, L. Rajendran and M.E.G. Lyons, *Int. J. Electrochem. Sci.*, 17 (2022) 220336.
34. B. Manimegalai, M.E.G. Lyons and L. Rajendran, *J. Electroanal. Chem.* 880 (2021) 114921.
35. R. Vanaja, P. Jeyabarathi, L. Rajendran and M.E.G. Lyons, *Int. J. Electrochem. Sci.*, 17 (2022) 220337.
36. R. Joy Salomi and L. Rajendran, *J. Electroanal. Chem.*, 918 (2022) 116429.